Electronic Supplementary Information

# How electrospray potentials can disrupt droplet microfluidics and how to prevent this

Andrea J. Peretzki,[a] Sabine Schmidt,[b] Elias Flachowsky,[a] Anish Das,[a] Renata F. Gerhardt[a] and Detlev Belder*[a]

[a] Institute of Analytical Chemistry, Leipzig University, Johannisallee 29, D-04103 Leipzig, Germany

[b] Center for Biotechnology and Biomedicine, Molecular Biological-Biochemical Processing Technology, Leipzig University, Deutscher Platz 5, D-04103 Leipzig, Germany



## 1 Flow and MS conditions

(SI-Table 1 on page 2)

**SI-Table 1:** Flow and MS conditions.

| Fig. | Droplet phase | Flow rate [µL/min] | Analyte | Continuous phase | Flow rate [µL/min] | $\Phi_{chip}$ [kV] | $\Phi_{counter}$ [kV] | $\Phi_{MS}$ [kV] | MS method |
|---|---|---|---|---|---|---|---|---|---|
| **2a** | ACN | 0.75 | 200 µM caffeine | PFD | 0.75 | +2.5 | 0 | 0 | Shimadzu<br>scan 180-230 m/z<br>event time 0.02 sec,<br>EIC 195 m/z |
| **2b** | 10 µM NH4OAc pH 7.4 | 1.00 | 100 µM AChCl | PFD | 0.50 | +2.7 | 0 | 0 | Shimadzu<br>scan 130-210 m/z<br>event time 0.02 sec,<br>EIC 146 m/z |
| **3a-c** | 10 µM NH4OAc pH 7.4 | 0.40 | - | PFD | 0.40 | varying | | | - |
| **4b-d** | MeOH/$H_2O$ 30/70 | 0.30 | - | PFD | 0.40 | +2.4 | 0 | 0 | - |
| **5b+c** | MeOH/$H_2O$ 30/70 | 0.50 | - | PFD | 0.90 | +2.8 | 0 | 0 | - |
| **6b+c** | MeOH/$H_2O$ 70/30 | 0.30 | - | PFD | 0.25 | +4.0 | 0 | 0 | - |
| **7a** | MeOH/$H_2O$ 65/35 | 0.50 | 50 µM C120 (Loop injection) | PFD | 0.60 | +3.0 | 0 | 0 | SIM 176 m/z<br>event time 0.08 sec |
| **7b** | MeOH/$H_2O$ 65/35 | 0.50 | 50 µM C120 (5 nL injection) | PFD | 0.30 | +3.0 | 0 | 0 | SIM 176 m/z<br>event time 0.08 sec |

## 2 Comparison of the orthogonal spray arrangement with counter electrode and spraying directly into the MS orifice

The detection of a stable and regular droplet trace works with both Chip-MS arrangement: the direct spraying into the MS orifice and with the MS placed orthogonally to the chip emitter. The baseline signal (a+c) shows the droplet trace without the analyte, in (b+d) an analyte peak eluting from the column is shown. For orthogonal infusion, both baseline signal and peak signal show a little higher intensity than with direct spaying. This small differences can also be due to a difference in distance between chip and MS or chip/MS and counter electrode. The S/N ratio for orthogonal infusion at 35.7 is slightly higher than for direct infusion at 33.3, which indicates that the orthogonal arrangement has no disadvantages in terms of sensitivity compared to direct spraying.

The droplets reflect a more uniform peak with orthogonal infusion than with direct spraying. The peak signal shows more spikes with direct spraying, which can be attributed to a higher oil entry in the in-line experiment.

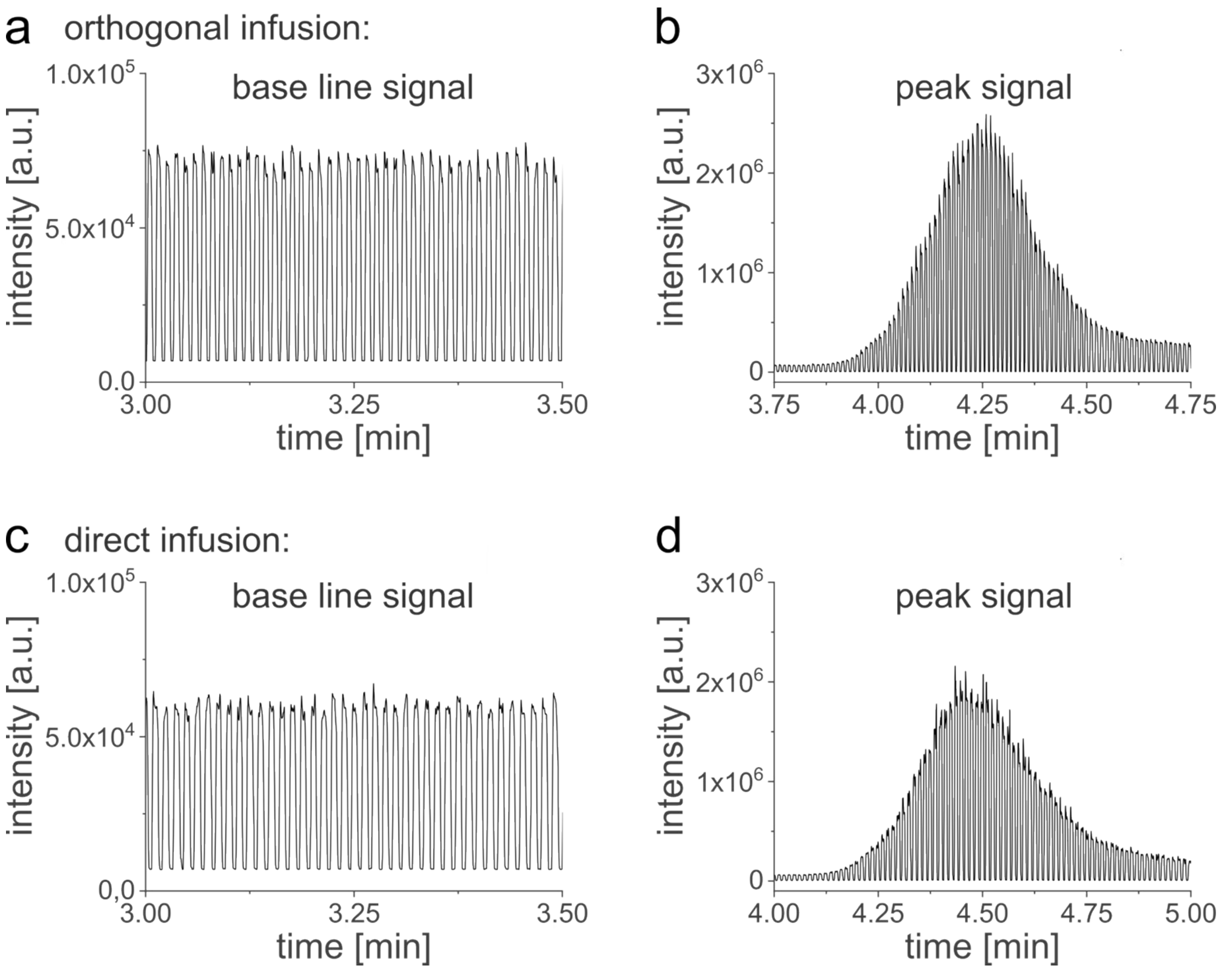


**SI-Figure 1:** Comparison of the orthogonal arrangement with counter electrode (a+b) and direct spraying from the chip into the MS orifice (c+d). Droplet phase: 0.50 µL/min MeOH/$H_2O$ 65/35 (v/v) +0.1% FA analyte: 50 µM pararosaniline (288 m/z), continuous oil phase: 0.50 µL/min perfluorodecalin, MS Shimadzu, Φ(Chip)= +2.5 kV, event time 0.03 sec.

# 3 Droplet formation under the influence of the electric field

**SI-Video-1:** Droplet formation under the influence of the potential alternating on/off every 5 sec.

Droplet phase: 10 µM $NH_4OAc$ pH 7.4, 0.40 µL/min, continuous oil phase: PFD, 0.40 µL/min, Φ(Chip)= +2.3 kV. Voltage off: the droplet formation was not affected. Droplets were formed with a regular frequency and shape. Voltage on: droplets were formed erratic, wet the channel wall, and merged in an uncontrolled manner. After switching off the voltage, the droplets were regularly generated again.

**SI-Table 2:** Droplet formation under the influence of different electrical potentials.

In this set of experiments, an electrospray was no longer generated at potentials lower than 2.0 kV. In further experiments (not shown) it was shown that at least 1.7 kV potential applied to the electrode was required to generate an electrospray. This indicates that droplets are already strongly influenced at much lower potentials (from 0.85 kV) than those required to generate an electrospray (at least 1.7 kV). Droplet phase: 0.4 µL/min MeOH/aqueous 10 mM $NH_4OAc$ 30/70 (v/v), continuous phase 0.4 µL/min PFD.

| Applied Potential | Electrospray generated | Effect on droplets observed | Microscopic photo |
|---|---|---|---|
| +2.33 kV | yes | strongly affected at any time | 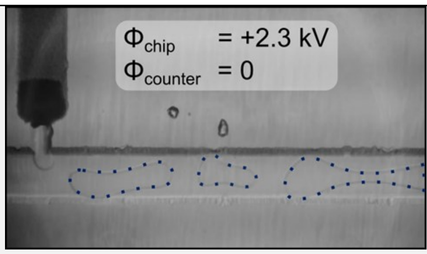 |
| +0.85 kV | no | about half of the droplets are strongly affected | 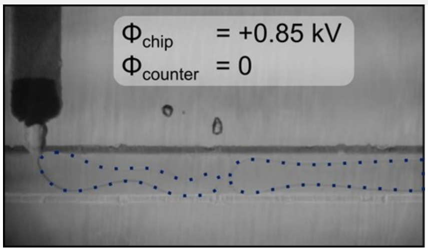 |
| +0.75 kV | no | Droplets are only slightly deformed, but not torn apart | 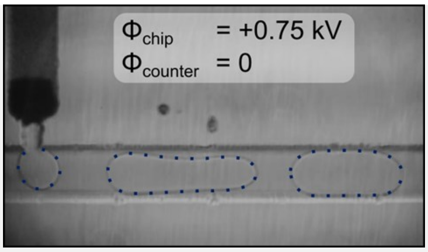 |
| 0 | no | Droplets are not affected at all | 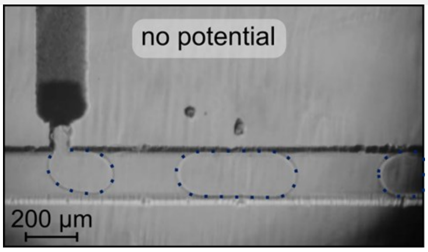 |

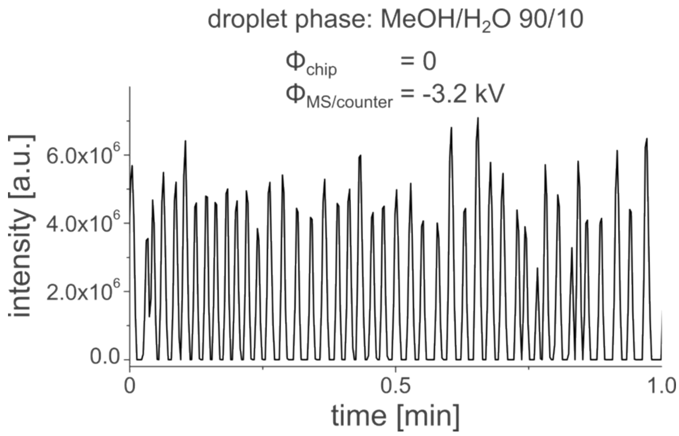


**SI-Figure 2:** Mass trace of on-chip generated droplets with electrical potential Φ applied to the counter electrode and the MS while the chip is on ground potential. Droplet formation and detection are stable. Droplet phase: 0.20 µL/min MeOH/$H_2O$ 90/10, analyte: 10 µM L-lysine, continuous phase: 0.50 µL/min perfluorodecalin, MS Agilent, scan 100-200 m/z, EIC 147 m/z, MS data rate 5.6 Hz.

# 4 Electrowetting

With the application of an electric potential across electrodes in a microfluidic device, a liquid droplet in the vicinity is attracted towards the electrodes that is biased. This phenomenon also causes the droplet to distort its shape leading to a decrease in apparent contact angle.[1] Due to the accumulation of charges at the droplet/surface interface the electrowetting phenomenon is observed.[2]

The electrowetting effect caused by the voltage induced change in the apparent contact angle of a droplet can be described by Lippmann & Young equation. Lippmann-Young equation[3] is defined as

$$\cos\theta = \cos\theta_0 + \frac{1}{2}\frac{\varepsilon_0\varepsilon_r}{\gamma d}V^2 \qquad (1)$$

Where $\cos\theta$ describes the droplet wetting and

$\theta$ = contact angle of electrowetting

$\theta_0$ = contact angle at 0 V

$\gamma$ = surface tension

$\varepsilon_0$ = vacuum permittivity

$\varepsilon_r$ = dielectric constant of the dielectric material

$d$ = thickness of the dielectric layer

$V$ = applied voltage

Assuming that the term $\frac{\varepsilon_0\varepsilon_r}{\gamma d}$ is constant $c$, the simplified form is

$$\cos\theta = \cos\theta_0 + \frac{c}{2}V^2 \qquad (2)$$

where $0° \leq \theta \leq 180°$ and $0° \leq \theta_0 \leq 180°$

as the contact angle is by its definition always in the range of 0° - 180°. Contact angles <90° represent a hydrophilic, wetting surface, >90° a hydrophobic, repellent surface. The minimum contact angle of 0° indicates an absolutely hydrophilic, completely wetting surface. With a maximum contact angle of 180° the surface is completely hydrophobic, so that a droplet on it forms an entirely spherical shape.[4,5]

The observed effects can be described qualitatively if the chip system is regarded as an "electrowetting experiment" as outlined in SI-Figure 3. The platinum electrode of the chip forms the electrode to which the high voltage is applied. The glass of the chip and the oil between the individual droplets act as a dielectric layer. The contact angle $\theta$ is the angle of the droplets relative to its base, i.e. the channel. The distance $d$, which describes the thickness of the dielectric layer, is in the chip experiment the distance between the electrode and the considered location of the droplet, for example the T-junction.

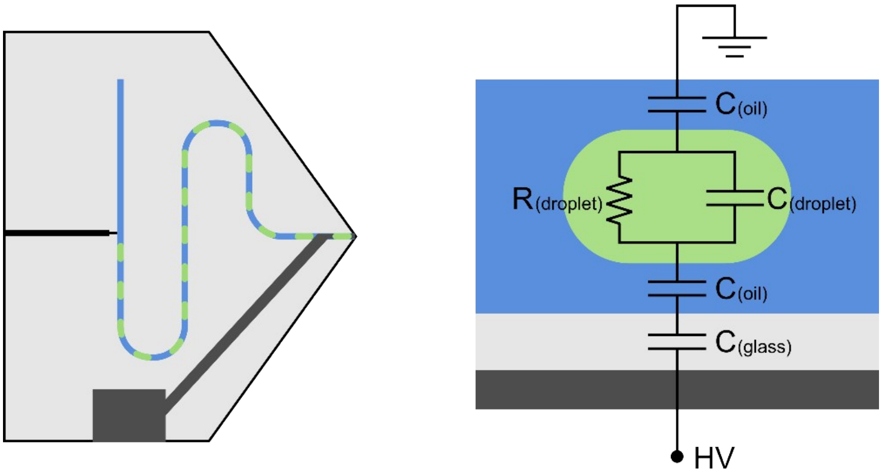


**SI-Figure 3:** Schematic drawing of the chip and the equivalent circuit diagram. Here the dielectric layer is treated as a Helmholtz capacitor.[6]

Applying the equation (2) for chip layout 1 and the different cases of potential under the assumption that the droplets do not move applies:

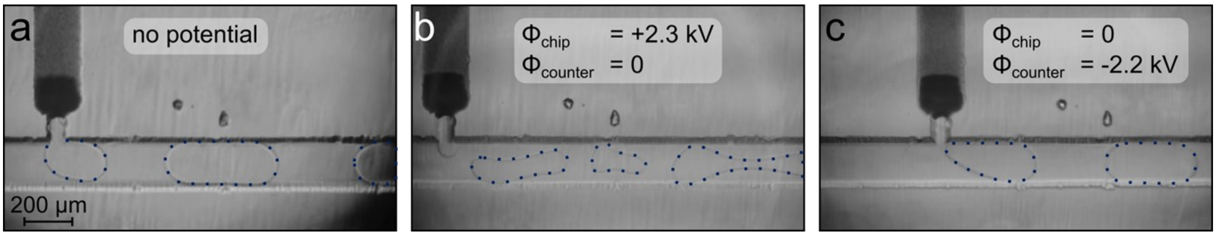


$V = 0$

$\cos\theta = \cos\theta_0 + \frac{c}{2}0^2$

$\cos\theta = \cos\theta_0 + 0$

$\cos\theta = \cos\theta_0$

as $0° \leq \theta, \theta_0 \leq 180°$

→ no wetting effects

$V = 2.3\ kV$

$\cos\theta = \cos\theta_0 + \frac{c}{2}(2300)^2$

$\cos\theta = \cos\theta_0 + 2.6 \times 10^6\ c$

$\cos\theta$ = droplet wetting is higher,

$\theta$ is lower

as $0° \leq \theta, \theta_0 \leq 180°$

→ the droplets are deformed

$V = 0$

$\cos\theta = \cos\theta_0$

as $0° \leq \theta, \theta_0 \leq 180°$

→ no wetting effects

For **chip layout 2** the linear distance $d$ and surface tension $\gamma$ is much higher than for chip layout 1. If $d$ and $\gamma$ are higher, the whole term $\frac{1}{2}\frac{\varepsilon_0\varepsilon_r}{\gamma d}V^2$ is much lower and approaching to zero, so again:

$\cos\theta = \cos\theta_0$

Which means that there is no change in the droplet contact angle and the droplet wetting.

However, since the droplets are in motion, the Maxwell stress tensor must also be considered.[7]

# 5 Investigated aqueous phase compositions

**SI-Table 3:** Investigated aqueous phase compositions under the influence of electrical potential applied to the chip.

| Composition of the droplet phase | Effect on droplets observed |
|---|---|
| **MeOH/ $NH_4OAc$ (10 mM, pH 7,4)** | |
| 0/100 (10 mM $NH_4OAc$) | affected |
| 30/70 (7 mM $NH_4OAc$) | affected |
| 50/50 (5 mM $NH_4OAc$) | affected |
| **MeOH/$H_2O$** | |
| 30/70 | affected |
| 50/50 | affected |
| 80/20 | affected |
| 0/100 | affected |
| 100/0 | not affected |
| **ACN 100 %** | not affected |

## 6 Evolution of the chip design

Further investigations showed that for both chip layouts 1a and b, the droplet generation was negatively influenced by applying a potential, but not for layout 2. Since the channel length of 1b is much longer than that of 2, and the distance between droplet generator and the emitter is much greater at 2 than at 1a+b, we conclude that the electric field propagates directly through the glass and not along the channels, which is supported by the theory of electrowetting (SI chapter 3).

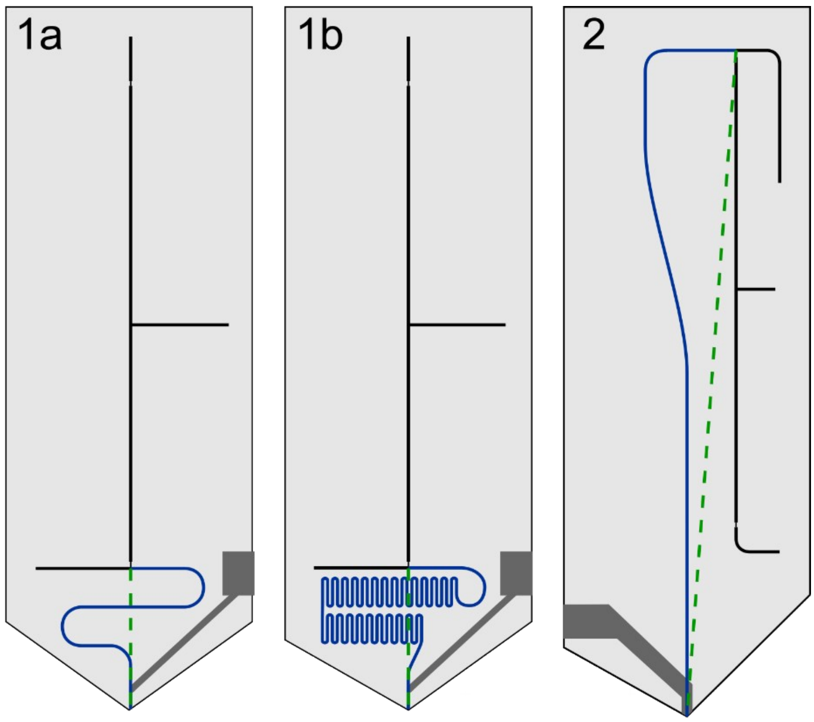


| | 1a | 1b | 2 |
|---|---|---|---|
| Channel length from T-junction to the tip | 36.2 mm | 173.8 mm | 79.8 mm |
| Linear distance between T-junction and the tip | 10.7 mm | 10.7 mm | 66.1 mm |
| Influence of potential on the droplets | yes | yes | no |

**SI-Figure 4:** Length of the droplet channels and linear distance between droplet generator and emitter tip for the initial design (1a) and with a prolonged channel (1b) and the changed design (2).

# 7 Formation of Droplet-Elctrospray with chiplayout 2 (“distancing approach”) with the electric potential on chip

**SI-Video-2 & SI-Video-3:** Video of the droplet-electrospray formation

**SI-Video-2:** The electrospray is formed periodically when a droplet reaches the emitter tip with the electrode. The oil that spaces the droplets from each other flows off at the outside of the tip towards the edge. Droplet phase: 0,5 µL/min MeOH/$H_2O$ 65/35 (v/v) + 0,1%FA, continuous oil phase: 0,3 µL/min PFD, Φ(Chip)= +2,4 kV.

**SI-Video-3:** In this experiment, one can see even more clearly how the oil drains off at the hydrophobic tip and is absorbed by the PTFE tape. SI-Figure-5 shows the corresponding droplet trace of the baseline (a) as well as a peak signal (b).

Droplet phase: 0,3 µL/min MeOH/$H_2O$ 65/35 (v/v) + 0,1%FA, continuous oil phase: 1,5 µL/min PFD, Φ(Chip)= +3,0 kV.

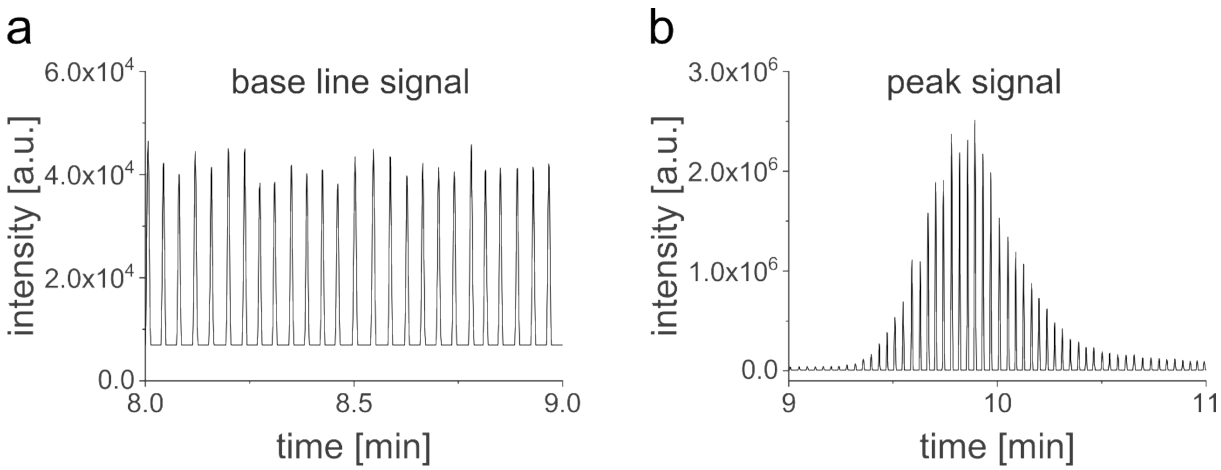


**SI-Figure 5:** The MS droplet signal associated with SI-Video 3. Droplet phase: 0,3 µL/min MeOH/$H_2O$ 65/35 (v/v) + 0,1% FA, continuous oil phase: 1,5 µL/min PFD, Φ(Chip)= +3,0 kV, MS signal: SIM mode 288 m/z.

## References

(1) Chatterjee, D.; Shepherd, H.; Garrell, R. L. Electromechanical model for actuating liquids in a two-plate droplet microfluidic device. *Lab Chip* **2009**, *9*, 1219–1229.

(2) Vallet, M.; Vallade, M.; Berge, B. Limiting phenomena for the spreading of water on polymer films by electrowetting. *Eur. Phys. J. B* **1999**, *11*, 583–591.

(3) Moon, H.; Cho, S. K.; Garrell, R. L.; Kim, C.-J. “C.”. Low voltage electrowetting-on-dielectric. *J. Appl. Phys.* **2002**, *92*, 4080–4087.

(4) Crick, C. R.; Parkin, I. P. Preparation and characterisation of super-hydrophobic surfaces. *Chem. Eur. J.* **2010**, *16*, 3568–3588.

(5) Jeevahan, J.; Chandrasekaran, M.; Britto Joseph, G.; Durairaj, R. B.; Mageshwaran, G. Superhydrophobic surfaces: a review on fundamentals, applications, and challenges. *J. Coat. Technol. Res.* **2018**, *15*, 231–250.

(6) Grahame, D. C. The electrical double layer and the theory of electrocapillarity. *Chem. Rev.* **1947**, *41*, 441–501.

(7) Mugele, F.; Baret, J.-C. Electrowetting: from basics to applications. *J. Phys.: Condens. Matter* **2005**, *17*, R705-R774.